



MODELS FOR SPACE ENVIRONMENTAL HAZARDS:

RADIATION

Issue II

January 31, 1964

Get DRA



FACILITY FORM 602

N71-71132
(ACCESSION NUMBER)

24
(PAGES)

CR-116548
(NASA CR OR TMX OR AD NUMBER)

(THRU)

NONE

(CODE)

(CATEGORY)

MODELS FOR SPACE ENVIRONMENTAL HAZARDS:

RADIATION

Issue II

January 31, 1964

Bellcomm, Inc.
Washington, D.C.

By H.J. Schulte
E.N. Shipley

TABLE OF CONTENTS

ABSTRACT

FORWARD

1.0 INTRODUCTION

2.0 GALACTIC COSMIC RAYS

- 2.1 Protons
- 2.2 Alpha Particles and Heavier Nuclei
- 2.3 Electrons and Gamma Rays

3.0 SOLAR COSMIC RAYS

- 3.1 Energy Spectrum and Composition
- 3.2 Model Solar Cosmic Ray Event
- 3.3 Composition of Model Event
- 3.4 Probability of Event
- 3.5 Electrons of High Energy
- 3.6 Solar Electromagnetic Radiation
- 3.7 Solar Wind

4.0 RADIATION TRAPPED IN EARTH'S MAGNETIC FIELD

- 4.1 Magnetically Trapped Protons
- 4.2 Magnetically Trapped Electrons

5.0 REFERENCES

ABSTRACT

Engineering design models are proposed for the penetrating radiation hazards of space. Charged particle and electromagnetic radiation in galactic and solar cosmic rays are discussed as well as trapped particles in natural and artificial belts.

FOREWORD

It is the purpose of this document to provide a set of models which will assist the Apollo designer in calculating the radiation hazard to the astronauts. In addition to the environment which is described here the spacecraft designer must also consider the trajectory and the effective vehicle shielding.

This compilation is believed to be complete and up to date. It is requested that omissions and corrections be brought to the authors' attention in order that the model may serve as a realistic standard.

Probable errors are quoted where it is reasonable to do so. Otherwise an uncertainty of a factor of two is to be understood.

This document is a revision of an earlier report issued as a Bellcomm Report on January 31, 1963, which it supercedes. Major changes have been made in Section 3, where exponential rigidity spectra have been used, and Section 4, where newer data on trapped radiation have been used.

MODELS FOR SPACE ENVIRONMENTAL HAZARDS: RADIATION

1.0 INTRODUCTION

The Apollo astronauts will be subject to penetrating radiation from three major sources. These are (1) solar flares, (2) Van Allen radiation belts, and (3) the galaxy. Galactic cosmic rays offer relatively little hazard. On the other hand, particulate radiation from the sun and energetic trapped electrons and protons in the Van Allen belts present a serious hazard. Models are given describing the fluxes and spectra and their time variation. For completeness, associated electromagnetic and other corpuscular radiations are also covered.

2.0 GALACTIC COSMIC RAYS

Galactic cosmic rays have been under study for many decades. Their sources have only recently been more or less agreed upon as the supernovae which are observed in the Milky Way Galaxy at the rate of one every few centuries. Interstellar magnetic fields provide storage and some acceleration which make the arrival of cosmic rays in the solar system essentially uniform in time and direction. Magnetic fields and fluctuations thereof near the earth cause direct observation to be less uniform.

Actual identification of the chief primary components as positively charged nuclei of various elements has only occurred in the past fifteen years. This was mainly because very high altitudes must be attained for such studies.

Biological and material effects of the primary galactic cosmic rays are rather minor even outside the earth's protective atmosphere and magnetic field.

2.1 Protons

The value of 2.0 ± 0.3 protons/cm² - sec for energy above 40 MeV is well known¹ for the flux at the time of maximum sunspot occurrence. At solar minimum the galactic flux may increase by a factor of two because at such times the sun's magnetic field provides less shielding to the earth. Above 10 BeV the integral energy spectrum varies as $kE^{-1.5}$.

2.2 Alpha Particles and Heavier Nuclei

The data of Johnson² for the composition of galactic cosmic radiation is given in Table I.

The energy spectrum (per nucleon) obeys roughly the same $E^{-1.5}$ law as quoted in 2.1 for protons. These relative abundances are sufficiently different from ordinary geologic, solar, or stellar abundances to aid in the aforementioned identification with supernovae.

| <u>Element</u> | <u>Relative Galactic Cosmic Ray Abundance</u> |
|---|---|
| Hydrogen | 1 |
| Helium | 7×10^{-2} |
| Lithium, Beryllium, Boron (collectively) | 4×10^{-4} |
| Carbon | 2×10^{-3} |
| Nitrogen | 1×10^{-3} |
| Oxygen | 2×10^{-3} |
| $10 \leq Z \leq 30$ | 1×10^{-3} |
| $Z \geq 30$ | $< 1 \times 10^{-6}$ |

Table I - Relative composition of galactic cosmic radiation

2.3 Electrons and Gamma Rays

No definite information is available on galactic cosmic ray components of these species. We assume the numbers are negligible. (See 3.5 - 3.7 on solar electrons, gamma rays, and the solar wind.)

3.0 SOLAR COSMIC RAYS

Beginning in 1956, occasional bursts of energetic particles originating on the sun have been observed in the vicinity of the earth. These bursts of particles, now commonly called solar cosmic ray events, were not detected in earlier years because of the lack of sufficiently advanced detection devices. Each burst lasts from one to four days, and consists primarily of protons and alpha particles, although heavier particles have been detected. Approximately 30 events of sufficient intensity to pose a possible radiation health problem to an astronaut have been observed. The largest event so far recorded had approximately 8×10^9 protons/cm² greater than 30 MeV.

Most of the solar cosmic ray events that have been seen so far have been detected by riometers, which are instruments which measure the absorption of galactic radio noise passing through the ionosphere. Because of the enhanced electron density produced by the ionizing particles from the sun, an increase in the absorption is observed when solar cosmic rays impinge on the atmosphere.

High energy protons (> 500 MeV) may produce neutrons when they are incident on the atmosphere. If there are sufficient high energy protons, an increase in counting rate can be observed by ground level neutron monitors. Direct observation of the incident protons and other particles has been made by payloads carried in balloons to altitudes above most of the earth's atmosphere, and in sounding rockets.

Since the advent of earth orbiting satellites, continuous direct measurements of solar cosmic ray particles above the atmosphere are possible. Satellites with eccentric orbits will make measurements outside of the magnetosphere, which shields the earth from many of the incident particles. Although a limited amount of data on a few solar cosmic ray events has been obtained with satellites so far, satellite experiments should provide future data far superior to that obtainable with other techniques.

All of the solar cosmic ray events have been preceded by a large solar flare occurring from 1 to 12 hours before the onset of the ionizing radiation at the earth. Solar flares are intense brightenings seen at optical wavelengths in the solar chromosphere in a localized region, usually located near a sunspot. The solar cosmic ray event of November 20, 1960, has been associated with an inferred flare located just behind the west limb of the sun³. In all other cases, solar cosmic ray events have been associated with solar flares on the visible hemisphere of the sun.

In the time interval 1956 to 1960, large solar flares (importance classes 2 and 3) occurred at the rate of roughly 1 per day, and smaller flares were seen at the rate of almost 10 per day. In the same 5 year time interval only 25 solar flares were associated with major solar cosmic ray events.

Inasmuch as a method of predicting an imminent solar cosmic ray event is highly desirable, a great effort is being made to determine which solar flares will be followed by a large particle flux. It has been found that a flare preceding a solar cosmic ray event is always accompanied by an intense broad band radio noise storm (Type IV radio noise storm) and that 43% of large flares accompanied by an intense Type IV noise storm were followed by solar cosmic rays⁴. Other flare properties, such as the fraction of the sunspot umbra covered by the flare, and the relative time history of the flare and the radio noise storm, can be used to improve the correlation between solar flares and subsequent solar cosmic ray events.

The frequency of solar flares, like other indications of solar activity, follows an approximate 11 year cycle. The last maximum occurred in 1958, and the next maximum is expected in about 1969. The period 1964-1965 corresponds to the minimum in solar activity, and the expected flare frequency is less than 1/10 that observed during the maximum of solar activity. Since all solar cosmic ray events are preceded by flares, it is generally assumed that periods of few solar flares will have few solar cosmic ray events.

3.1 Solar Cosmic Ray Energy Spectrum and Composition

The energy spectrum of solar cosmic rays can be measured directly by nuclear emulsions flown in balloons and sounding rockets. The flight of sounding rockets is so brief that only the most intense portion of the spectrum can be observed, while balloons are instruments limited to relatively high energy particles because of the shielding of the residual atmosphere above the balloon. In addition, the earth's magnetosphere deflects charged particles with the result that, except over the magnetic poles, the low energy portion of the spectrum is missing. Sounding rockets and balloons provide coverage only for a few minutes and a few hours, respectively, after they are launched. In general, launches are made after the start of an event has been detected by other means, so that these detectors commonly are unavailable in the early part of an event.

The energy spectrum of many solar cosmic ray events has been inferred from the relative effects produced in neutron monitors, which are sensitive to protons with energy > 500 MeV, and in riometers which are most sensitive to protons having an energy of about 30 MeV. In other cases, the spectrum is inferred from the variation in absorption observed by riometers located at different geomagnetic latitudes, since the earth's magnetic field has a decreasing shielding effect as one moves from the equator to the poles.

It has been observed that the energy spectrum of solar cosmic rays changes significantly during the course of an event. Those particles which arrive first tend to have a higher energy than those which arrive later.

Originally it was felt that at a particular time during the event the energy spectrum of solar cosmic rays could be represented as a power law

$$N(> E) = kE^{-n} \quad (1)$$

where E is the particle energy, $N(> E)$ is the number of particles having energy greater than E , and k and n are adjustable parameters. Later it was observed that a different value of n was required for high energies than for low energies, and a more accurate representation of the particle flux is given by an exponential rigidity spectrum²

$$N(> R) = J_0 e^{-R/R_0} \quad (2)$$

R is the rigidity of the particle

$$R = \frac{pc}{Ze}$$

where p is the momentum, c is the velocity of light, Ze is the nuclear charge, R_0 and J_0 are parameters, and $N(> R)$ is the number of particles having a rigidity greater than R . R_0 decreases during the course of an event corresponding to the decrease in energy of the particles, and J_0 passes through a maximum.

The composition of solar cosmic rays has been studied using nuclear emulsions flown in sounding rockets and in balloons. Frier and Webber³ have found that in a large fraction of the observed events, protons and alpha particles have identical exponential rigidity spectra, so that equal rigidity intervals have equal numbers of protons and alpha particles. The relative abundances of different particles are often expressed for equal energy per nucleon intervals. If protons and alpha particles had identical exponential rigidity spectra of the form of equation (2), with $R_0 = 100$ MV, the proton to alpha particle ratio for equal kinetic energy/nucleon intervals at 50 MeV/nucleon would be 11/1.

In addition to the variation that is observed during the course of each event, one event differs from another in total flux, spectrum, and composition. In most cases, the solar cosmic ray particles arrive at the earth isotropically. Neutron monitors can be used to detect anisotropy, and some events have an appreciable anisotropy early in the event⁶. The duration of this effect is several hours.

3.2 Model Solar Cosmic Ray Event

Bailey⁷ has synthesized the time history of a typical solar cosmic ray event from proton spectral measurements for events occurring before 1961. This synthesis has been adopted here as the basis of a model solar cosmic ray event.

The curves given by Bailey can be closely approximated by exponential rigidity spectra of the form of equation (2). The parameters R_0 and J_0 for such a fit are listed in Table II for various times after the associated solar flare, and they are plotted in Figure 1. Proton energy spectra corresponding to the exponential rigidity spectra are given in Figure 2.

| <u>Time after flare</u> <u>(hours)</u> | <u>J_0, particles/cm²-</u> <u>sec-steradian</u> | <u>R_0, MV (million volts)</u> |
|---|--|---|
| 1/2 | 0.4 | 718 |
| 1 | 3.5 | 514 |
| 2 | 75. | 254 |
| 4 | 1.7×10^3 | 145 |
| 8 | 1.1×10^4 | 107 |
| 16 | 3×10^4 | 84 |
| 32 | 6×10^4 | 70 |
| 64 | 4×10^4 | 70 |
| 128 | 9×10^3 | 70 |

TABLE II - Parameters for the exponential rigidity spectra of the model solar cosmic ray event.

The rigidity spectra apply directly to protons and alpha particles, so that there are equal numbers of protons and alphas in the same rigidity interval. Heavier elements have the same general spectrum but smaller intensities as discussed in section 3.3.

The spectrum of protons time integrated over the entire event is shown in Figure 3, and may be represented by the relation

$$N(>R) = 12 \times 10^{10} e^{-R/80} \quad (3)$$

where $N(>R)$ is the number of protons/cm² with rigidity greater than R , in MV (million volts). The same expression applies to alpha particles.

It is assumed that the model flare is a completely isotropic event. With this assumption, intensities quoted in terms of particles/cm² steradian or particles/cm² differ by a factor of 4π .

3.3 Composition of Model Event

Recent studies using nuclear emulsions have shown that the spectrum of heavy particles in solar cosmic rays have the same rigidity dependence as do protons and alpha particles. The relative fluxes of hydrogen, helium and heavier elements for equal rigidity intervals were obtained from the data of Biswas et al⁸, and are in Table III. To obtain the correct rigidity spectrum for any element, the intensities J_0 in Table II or the factor 12×10^{10} in equation (3) must be multiplied by the appropriate relative intensity from Table III.

| <u>Element</u> | <u>Relative Flux</u> |
|----------------------|----------------------|
| Hydrogen | 1 |
| Helium | 1 |
| Beryllium and Boron | $< 2 \times 10^{-4}$ |
| Carbon | 5×10^{-3} |
| Nitrogen | 1×10^{-3} |
| Oxygen | 9×10^{-3} |
| Fluorine | $< 3 \times 10^{-4}$ |
| Neon | 1×10^{-3} |
| Sodium through Argon | 1×10^{-3} |

TABLE III - Relative fluxes of various elements in solar cosmic rays for equal rigidity intervals.

3.4 Probability of Event

The probability of occurrence of a solar cosmic ray event as a function of its size has been studied previously⁹. The results of that study are reproduced in Figure 4. This frequency curve refers to the rate of occurrence of events during a maximum of the solar cycle. The frequency of events is expected to be less at other times. The sequences of events which occurred on August 29 and 31, 1957; on August 22 and 26, 1958; on July 10, 14 and 16, 1959; on November 12, 15, and 20, 1960; and in the interval July 11 to 20, 1961 have each been treated as single events. The intensity of the composite has been taken equal to the sum of the intensities of the events in the sequence.

Numerous events which were not included in the study made in Reference 9, have been observed¹⁰. These events have not been included because their size estimates are less well established. Inclusion of these events with the existing estimates would have no appreciable effect on the size-frequency curve above size of 5×10^6 protons/cm², but would approximately double the frequency of events exceeding 1×10^7 protons/cm².

With the use of the results of Reference 9, the probability per day, P, of having an event with a total flux of protons larger than N is given by

$$P(N) = .0022 (10 - \log_{10} N) \quad (4)$$

$$N < 10^{10} \text{ protons/cm}^2$$

where N is the number of protons/cm² with energy above 30 MeV. Equation (4) is plotted in Figure 4. A proton energy of 30 MeV corresponds to a rigidity of 239.2 MV.

It is assumed that the spectrum for an event of any size is similar to the spectrum given in Section 3.2, which has a total flux of 6×10^9 protons/cm² above 30 MeV. It should be assumed that the intensities at any time for an event of arbitrary size is proportional to the intensity given in Section 3.2.

The event sizes in this section refer to the number of protons in the event. In all cases, an equal number of alpha particles with the same rigidity spectrum should be used.

3.5 Solar Electrons (High Energy)

We base the following model on only one experiment, that of Meyer and Vogt¹¹.

Electrons having energies between 100 and 1300 MeV were detected on July 22, 1961, at the same time as primary protons which followed the solar flare of July 20. The result was $3.7 \pm 0.5 \times 10^{-2}$ electrons/cm²-sec-steradian. The solar cosmic ray event of July 20 had an integrated flux of 2.5×10^8 protons/cm², so that this event was of moderate intensity.

3.6 Solar Electromagnetic Radiation

Brief bursts (~5 minute duration during solar flares) of solar gamma radiation in the 20 to 500 keV energy region have been observed on two occasions^{12, 13}. Flux rates of approximately 10^7 keV/cm²sec were measured, implying ~100 photons/cm²sec.

Thus we adopt as an upper limit to the expected gamma ray flux from a solar flare.

$$\frac{N_{\text{photon}}}{N_{\text{proton}}} < 3 \times 10^{-5}$$

with photon energy from 0.1 to 1.0 MeV.

For lower photon energies Friedman¹⁴ states that the following energy radiation, essentially continuous in time, is typical for a quiet sun:

| <u>Wave length (Angstrom Units)</u> | <u>Energy flux at 1 astronomical unit (erg/cm²sec)</u> |
|--|---|
| $\lambda < 105$ | 0.8 |
| < 1200 | 3.8 |
| < 1600 | 20.0 |
| Entire spectrum, including visible light | 1.4×10^6 |

3.7 Solar Wind

The solar wind is the name commonly applied to the two-component plasma which is observed at earth distances from the sun. It is always present except that variations in flux of factors of ten or more are measured and these contribute to the variations which are observed in the cislunar magnetic field. The solar wind is far from completely measured and understood at this time.

Most of the reliable measurements^{15, 16} have yielded proton and electron densities of the order of 10 particles/cm³. The bulk velocity is about 3×10^7 cm/sec, indicating a flux of the order of 3×10^8 particles/cm² sec and a mean proton kinetic energy of about 500 eV.

Reports of the Mariner II probe¹⁷ are in good agreement with these values.

4.0 RADIATION TRAPPED IN THE EARTH'S MAGNETIC FIELD

Both protons and electrons whose energies spread over several decades are observed^{18, 19} in the radiation belts first discovered by Van Allen. The range of altitude is also large, extending from a few hundred kilometers to ten or more earth radii.

When the trapped particle density is described in ordinary spherical geographic coordinates there is considerable irregularity, owing to the departure of the shape of the earth's magnetic field from that of a simple dipole. An adequate representation of the field has been achieved by the 48 term expansion of Jensen and Cain²⁰. Using this model of the field, McIlwain²¹ has developed the B-L coordinate system which produces a great simplification of the trapped particle density description. Two coordinates suffice: B, which is the magnitude of the magnetic induction, and L, which in a dipole field would be the equatorial distance to the field line which includes the point in question. L is actually defined in terms of the integral invariant which describes the helical motion of the charged particle as it spirals around a line of force from the southern to the northern mirror point and return.

A further transformation which has been described by McIlwain permits a more pictorial description of the particle density. This is a second two-dimensional display, in the coordinates R- λ of an ideal dipole field when R is the radial distance from the center of the earth and λ is the geomagnetic latitude. The plots of Figure 5 and 6 are in these coordinates. In this plot the earth's surface is rough, with irregularities of a few hundred kilometers as a result of the transformation which makes the contours of constant trapped particle density smooth. Thus, to picture the radiation belts, one first transforms to B-L coordinates using the actual magnetic field expansion and the integral invariant description of the particle motion. Next, a second transform to R- λ coordinates may be made to achieve a more intuitive description of the belts. This simple transformation is given by $R = L \cos^2 \lambda$, $B = \frac{M}{R^3} \sqrt{4 - \frac{3R}{L}}$

where M is the dipole moment of the earth's field.

The B-L representation of the trapped particle fluxes is useful in estimating the radiation dose received by space vehicles. Given the trajectory in geographic coordinates, one transforms to B-L coordinates, in which the particle flux is known. Thus, even those geographic regions of the vehicle trajectory where the flux is not directly measured are filled in because of the contraction from a three to a two dimensional description.

In general, the belt hazard is considered serious for certain circumstances. However, moderate shielding (2 gm/cm^2), careful selection of trajectories, or fast passage make lunar missions quite reasonable. Similarly, very low or very high altitude orbiting satellites are relatively safe but repeated passage through the belts in eccentric orbits or continuous travel in near-circular orbits at medium altitude is quite hazardous. For example, the unshielded dose rate at the heart of the belts is of the order of rads per second. With 5 gm/cm^2 it is still about one rad per hour, mostly from bremsstrahlung.

The decay of the proton population is essentially nil. The electron data cited below is for January 1, 1963. No good evaluation of the decay since then is available. It is dependent upon L , magnetic latitude, and energy in a way which is not well understood, but which is the subject of continuing study. In the heart of the belts, where a translunar trajectory dose is determined, the variation in the past year is small. We shall ignore it.

4.1 Magnetically Trapped Protons

As seen in Figure 5 the protons are concentrated at relatively low altitudes. Their peak intensity lies near 1.5 earth radii and there have been only small variations in flux values noted over several years. The protons are believed by some¹⁸ to be the result of neutron decay above the atmosphere.


Excellent detailed $R-\lambda$ plots for proton energies from 40 to 110 MeV have been published by McIlwain²², from which Figure 5 is adopted. The energy spectra are not yet thoroughly mapped but a recent emulsion study by Heckman and Armstrong²³ gives useful results from South Atlantic ballistic missile flights. They give a differential spectrum which is roughly flat from 10 to 100 MeV, then bends over to about an E^{-2} spectrum at 500 MeV.


4.2 Magnetically Trapped Electrons

The rough spatial distribution of electrons above 0.5 MeV is shown in Figure 6. Again the excellent article by McIlwain²² is suggested. There are two belts: the lower centered on about 1.3 earth radii and the outer peaked at about 4.0 earth radii. The inner belt is relatively free of short

term fluctuations although there is a slow decay with a mean life of about a month above $L = 1.5$. The decay rate is somewhat larger at higher L values. The electrons at lower L values (1.2 - 2.0 earth radii) are believed to be chiefly the remnants of various high altitude nuclear tests which occurred in the summer and fall of 1962. They represent the main radiation belt hazard to space vehicles. Their spectra has not yet been thoroughly mapped either, although some measurements have been made²⁴ and a general estimate of the spatial variation has been sketched in qualitative terms²⁵. The spectra in general have a fission-like high energy tail up to several MeV with a peak near 1.5 MeV for some locations.

The outer electron belt is very poorly studied at this time. One can say that the fluxes are less by two to three orders of magnitude than at the heart of the inner belt near the equator. The outer belt flux is relatively constant with variation in magnetic latitude along a constant L line in contrast to that of the inner belt which falls off by two orders of magnitude or so from the magnetic equator to 30° latitude. Time fluctuations of a factor of 20 are observed in the outer belt flux in the space of a day or two.


H.J. Schulte


E.N. Shipley

1112-HJS-SP
ENS

5.0 REFERENCES

1. F.S. Johnson, Satellite Environment Handbook, (Stanford University Press, Stanford, 1961) p. 70.
2. Ibid, p. 65.
3. H.M. Malitson, Solar Proton Manual (NASA TR R-169, edited by F.B. McDonald) Appendix A, p. 98.
4. B. Bell, Smithsonian Contributions to Astrophysics, 8, 119 (1963).
5. P.S. Freier and W.R. Webber, J. Geophys. Research 68, 1605 (1963).
6. K.G. McCracken, J. Geophys. Research 67, 435 (1962).
7. D.K. Bailey, J. Geophys. Research 67, 391 (1962).
8. S. Biswas, C.E. Fichtel, D.E. Guss and C.J. Waddington, J. Geophys. Research 68, 3109 (1962).
9. D.B. James, M.A. Leibowitz, and H.J. Schulte, The Radiation Environment of Apollo, Bellcomm, Inc. Report, October 21, 1963.
10. C.S. Warwick and M.W. Hauritz, J. Geophys. Research 67, 1317 (1962).
11. P. Meyer and R. Vogt, Phys. Rev. Letters 8, 387 (1962).
12. C.E. Fichtel, Proceedings of Gatlinburg Symposium on Radiation Hazards in Space (T1D-7652, 1962) p. 33.
13. L.E. Peterson and J.R. Winkler, J. Geophys. Research 64, 697 (1959).
14. H. Friedman, Astronautics, Vol. 7, #8. p. 14 (August 1962).
15. B. Rossi, Space Research III (Interscience Publishers, New York, 1963, edited by W. Priester) pp. 529-539.
16. J.H. Piddington, Planetary and Space Science 9, 305 (1962).
17. M. Neugebauer and C.W. Snyder, Science 138, 1095 (1962).
18. W.N. Hess, Space Science Review 1, 278 (1962).
19. F.S. Johnson, Satellite Environment Handbook, (Stanford University Press, Stanford, 1961) p. 54-58.
20. D.C. Jensen and J.G. Cain, J. Geophys. Research 67, 3568 (1962).

21. C.E. McIlwain, J. Geophys. Research 66, 3681 (1961).
22. C.E. McIlwain, Science 142, 355 (1963).
23. H.H. Heckman and A.H. Armstrong, J. Geophys. Research 67, 1255 (1962).
24. H.I. West, Jr., L.G. Mann and S.D. Bloom, Spectra and Fluxes of Electrons Trapped in the Earth's Magnetic Field Following Recent High Altitude Nuclear Bursts, UCRL 7309, Rev. I (1963).
25. W.L. Brown, J.D. Gabbe and W. Rosenzweig, Bell System Technical Journal XLII, 1505 (1963).

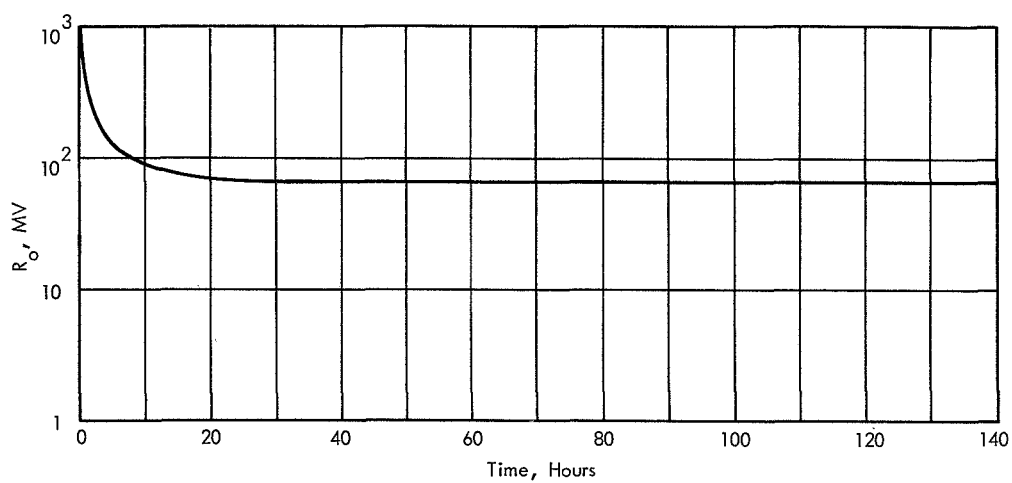
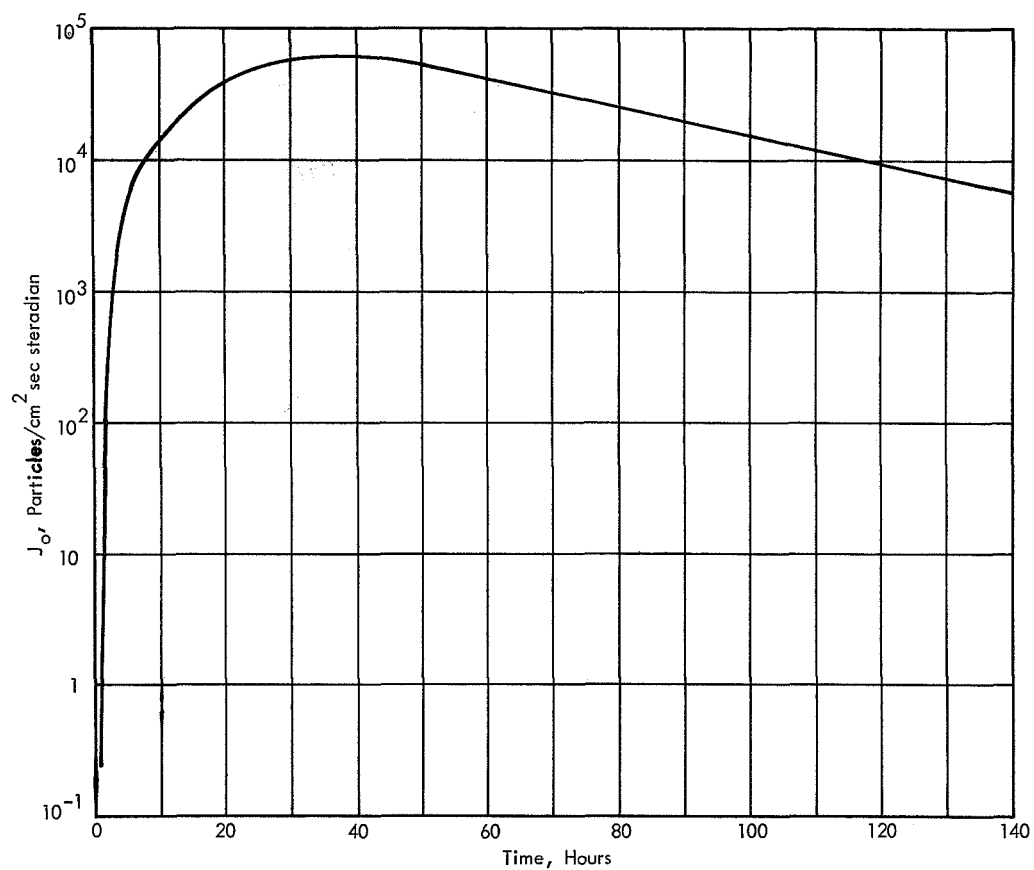


FIGURE 1. BEHAVIOR OF EXPONENTIAL RIGIDITY
PARAMETERS AS A FUNCTION OF TIME.
THE SPECTRUM OF PROTONS OR ALPHA
PARTICLES IN THE MODEL SOLAR COSMIC
RAY EVENT IS GIVEN BY $N(>R) = J_0 \exp(-R/R_0)$

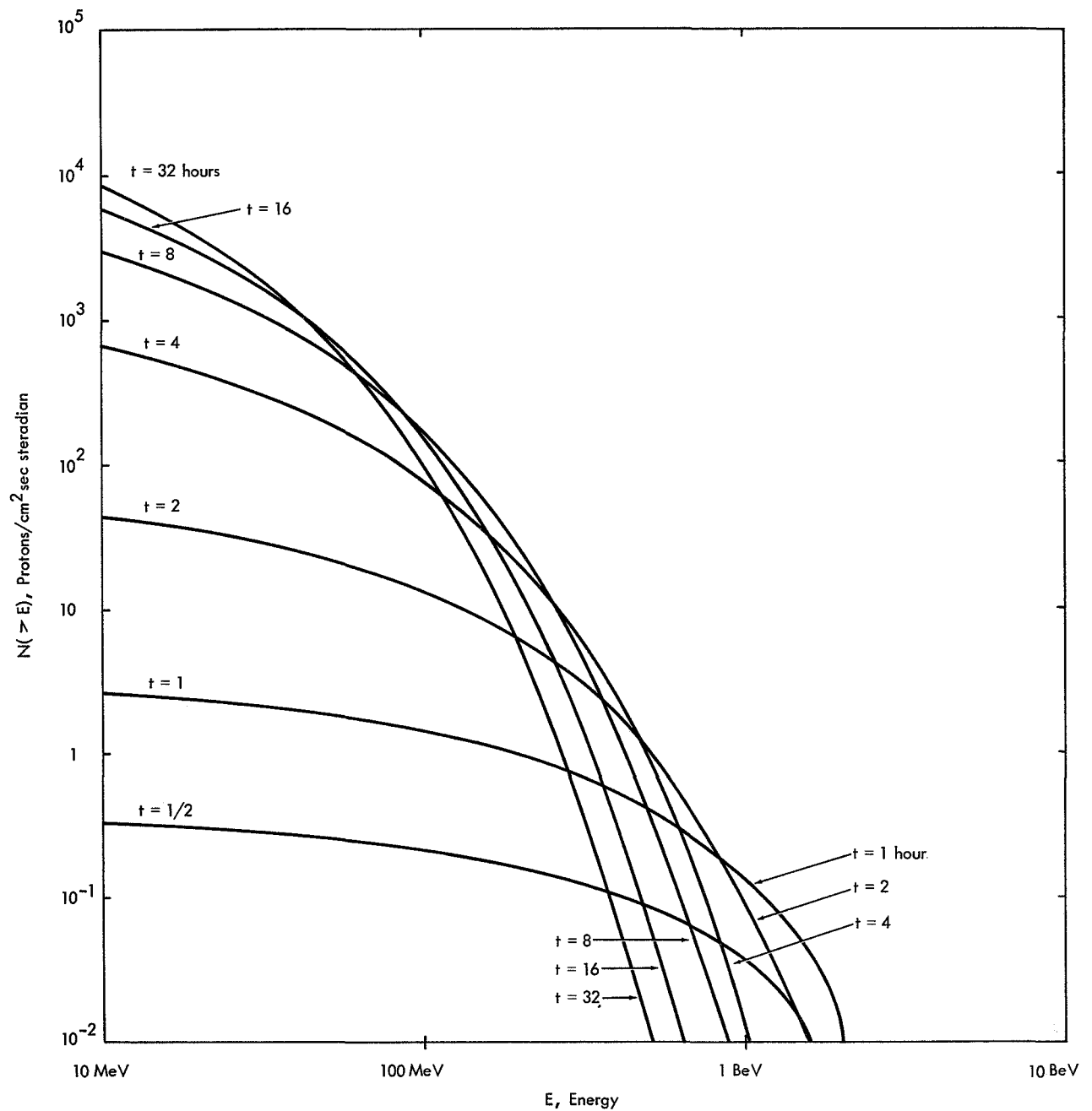


FIGURE 2. PROTON ENERGY SPECTRUM OF THE MODEL SOLAR COSMIC RAY EVENT. THE NUMBER OF PROTONS HAVING ENERGY GREATER THAN E IS PLOTTED FOR VARIOUS TIMES AFTER THE ASSOCIATED SOLAR FLARE.

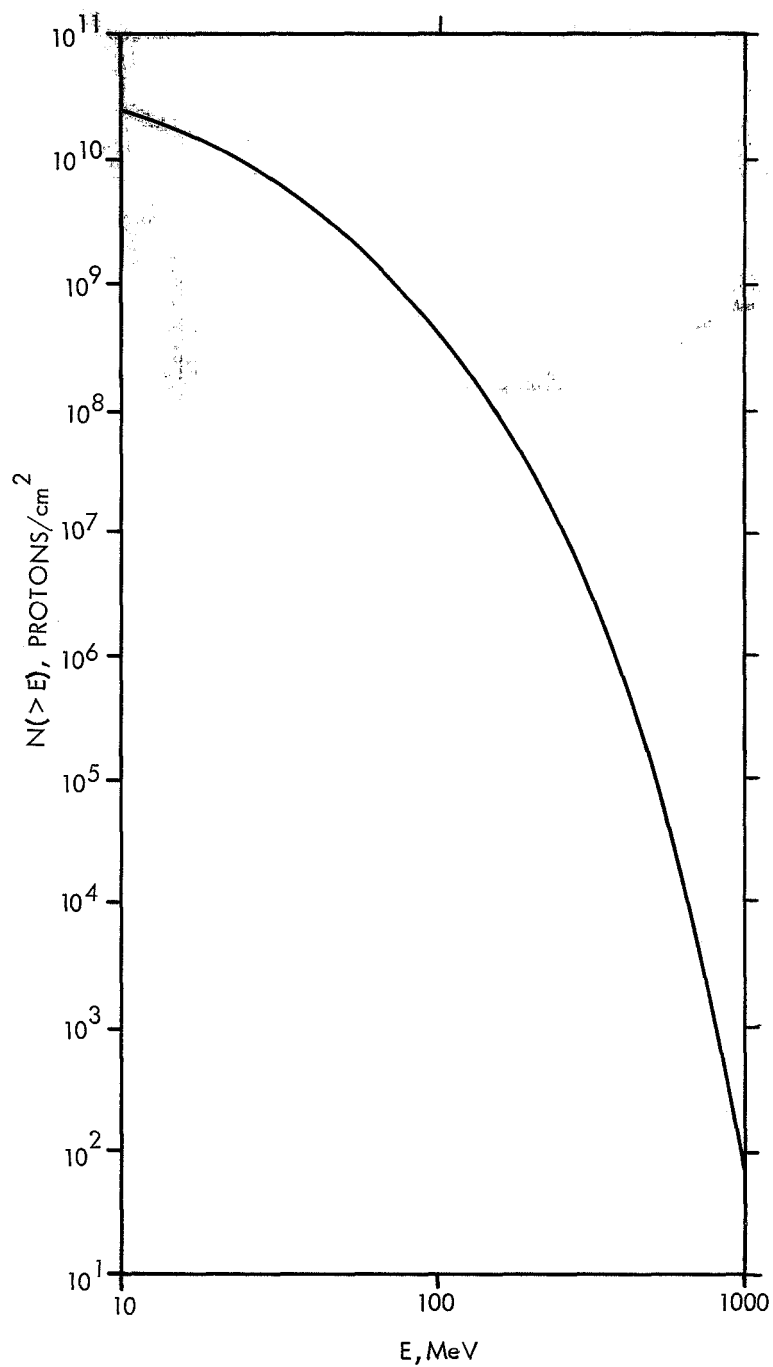


FIGURE 3. PROTON ENERGY SPECTRUM OF THE MODEL SOLAR COSMIC RAY EVENT, INTEGRATED OVER TIME FOR THE ENTIRE EVENT. THE NUMBER OF PROTONS WITH ENERGY GREATER THAN E IS PLOTTED AGAINST E.

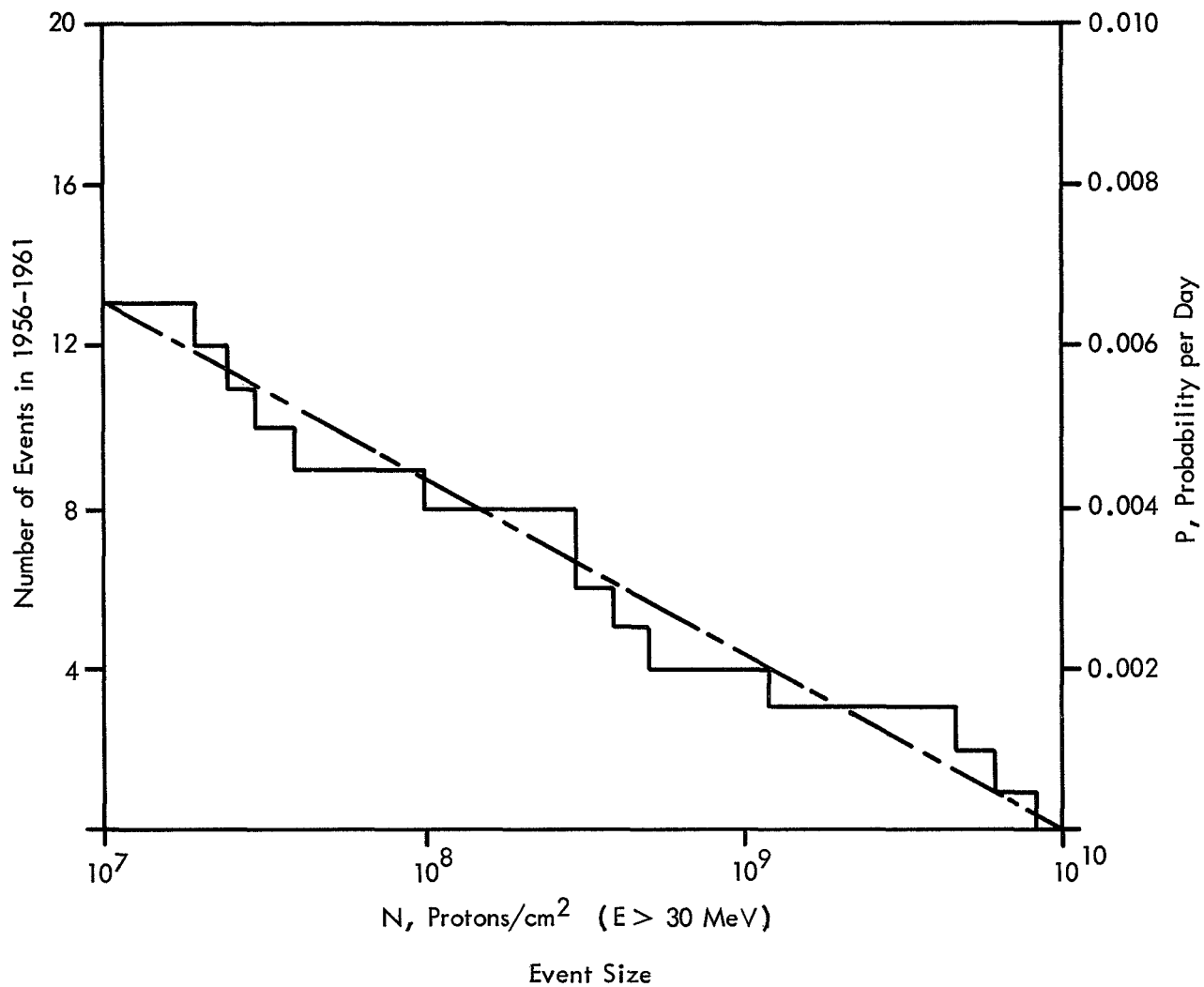


FIGURE 4. NUMBER OF SOLAR COSMIC RAY EVENTS IN 2000 DAYS (1956 - 1961) WITH SIZE GREATER THAN N. THE RIGHT HAND SCALE GIVES THE PROBABILITY PER DAY FOR THE OCCURENCE OF AN EVENT HAVING A SIZE GREATER THAN N. THE DASHED LINE IS THE RELATION $P(N) = 0.0022 (10 - \log_{10} N)$.

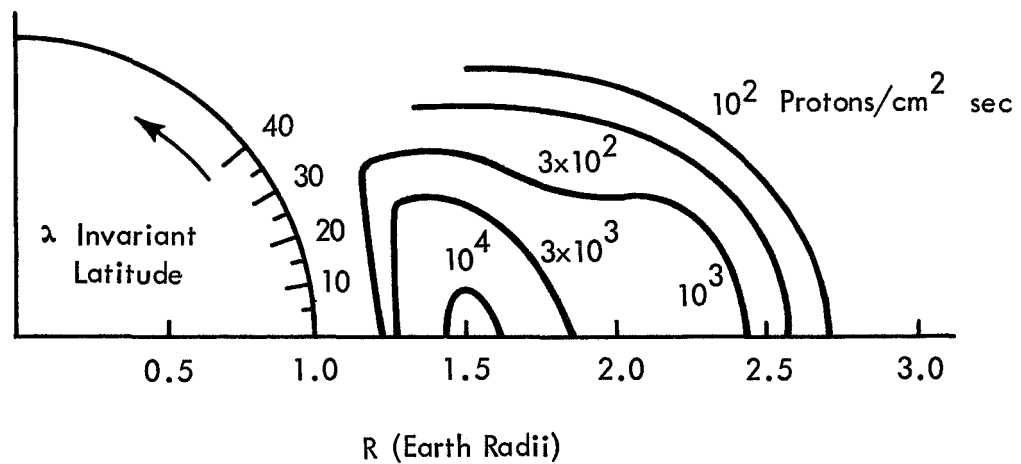


FIGURE 5 CONTOURS OF CONSTANT OMNIDIRECTIONAL
 PROTON FLUX (40 TO 110 MeV) - IN R - λ SPACE
 SEE C.E. McILWAIN, SCIENCE 142, 356 (1963)

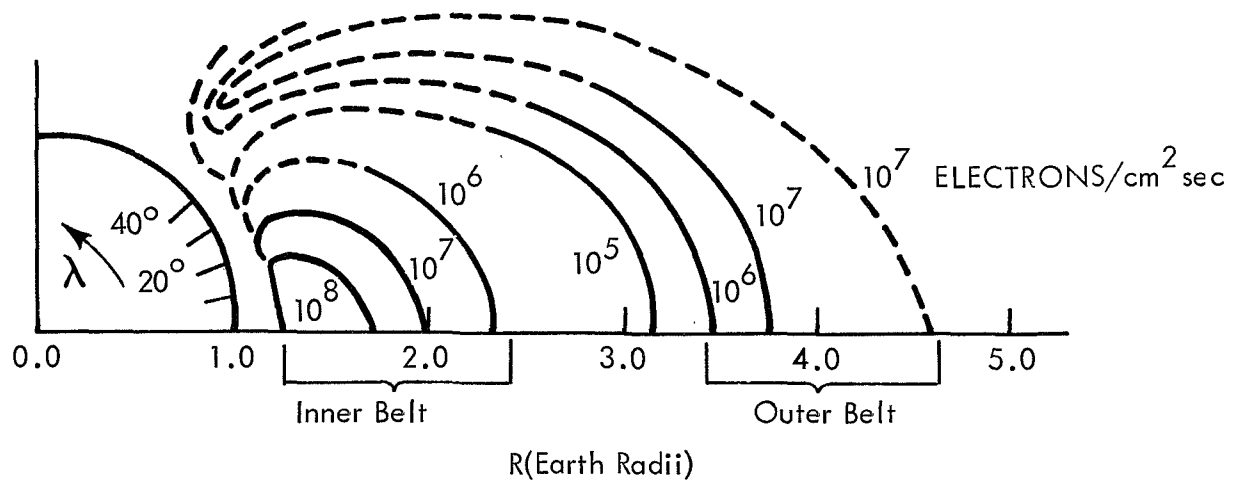


FIGURE 6 CONTOURS OF CONSTANT OMNIDIRECTIONAL ELECTRON FLUX ($E > 0.5$ MeV) IN R- λ SPACE. SEE C.E. McILWAIN, SCIENCE 142, 357 (1963)

